طريقة أجزاء متناهية منفصلة الطبقات للوائح الأسطوانية

محمد العجمي

قسم الهندسة الميكانيكية، كلية الهندسة والبترول، جامعة الكويت

الخلاصـة

يقدم هذا البحث نموذج جديد لطرق الأجزاء المتناهية للوائح الاسطوانية المركبة والرقيقة ومعتدلة السماكة بالاعتماد على نظرية الاستطالة من الدرجة الأولى. وعدد درجات الحرية كل جزء متناهي هي عشرون درجة ومبنية على فرضية الإجهاد السطحي وموزعة على درجات استطالة معرفة بالتوازي مع أسطح اللوائح وأخرى عمودية باتجاه قطر الأسطوانة. كما تم تطبيق طريقة المجال متسق للتأكد من أن الأجزاء المتناهية خالية من التصلب القصري الناتج عن نموذج الاستطالة وفرضياتها والذي نجح بإزالة التصلب عن طريق حذف بعض أجزاء الغير منسجمة والمستخدمة كنموذج للاستطالة. وأخيرا، تم التحقق من صحة النموذج الجديد بمقارنتها مع مجموعة من نتائج الأبحاث المنشورة سابقا.

A discrete layer finite element model for cylindrical shells

Mohammed A. Al-Ajmi

Mechanical Engineering Department, Kuwait University, P.O. Box 5969, Safat 13060, Kuwait.

m.alajmi@ku.edu.kw

ABSTRACT

This paper presents a new discrete layer finite element method modeling thin and moderately thick orthotropic and laminated composite cylindrical shells. The element formulation is based on the first order shear deformation theory of shells. A twenty-degrees-of-freedom plane stress element is utilized and modeled with in-plane displacements defined at the interfaces of the element layers in addition to the radial displacement. A field consistency approach is implemented to insure that the element is free from locking due to membrane tangential, shear and transverse shear strains. The field consistency approach used eliminates inconsistent terms from the original displacement shape functions that correspond to the targeted strains. The new element is validated through a series of benchmark problems and has shown accurate and fast converging results.

Keywords: Discrete layer; finite element; locking; shells

INTRODUCTION

Shells are major structural elements in diverse fields of engineering technology such as automotive, aerospace and civil construction. The simulation of complex structures, including shells, is a mandatory step in engineering design and the finite element method is the best computational procedure known to date that can serve this purpose. The finite elements of shells started with the facet shell element (Hrennikoff & Tezcan, 1966; Zienkiewicz & Cheung, 1966), where the shell surface is treated as an assembly of flat plate elements. This method lacks the coupling between bending and membrane within each element and requires coordinate transformation to derive the element mass and stiffness matrices. Thus, to overcome the disadvantages of the facet shell elements, research efforts continued toward deriving curved shell elements that are based on shell theories, and the initial efforts resulted in the first known thin shell finite elements by Bogner *et al.* (1967) and Connor & Brebbia (1967). Another family of elements is the degenerated shell elements developed by Ahmad *et al.* (1970), which discretize the three dimensional solid element in terms of mid-surface

nodal variables. The last well established type of shell elements is known as the solid shell element (Ausserer & Lee, 1988). In this approach, the shell element is modeled either as a 3-D solid element with three displacement components per node or a 2-D solid element with six vector components per node defined over a mid-surface or a reference surface.

A numerical problem known by *locking*, is usually encountered in finite element modeling for which some parts of the element stiffness matrix have unreasonably high values under specific loading and/or geometric conditions, resultsing in an overall *stiff* element. For structural mechanics type of problems, the finite element locking phenomenon is found mostly in shear deformable structures with strong appearance in curved structures.

Several methods have been developed to alleviate locking in shell elements such as the assumed strain method, which is a very effective way that has been successfully applied to overcome locking problems in curved elements. One of the earliest works in the assumed strain approach was done by Ashwell & Sabir (1972) to derive independent strain functions for thin cylindrical shells including explicit rigid body modes. Their idea was extended by many authors such as, for example, Djoudi & Bahai (2004), who used a different thin shallow shell theory. The success of the original approach was followed by many efforts, such as the work done by MacNeal (1982) to derive bilinear shell elements, and by Dvorkin & Bathe (1984) to derive a class of successful degenerated shell elements known by MITC elements. Consequently, The enhanced assumed strain method, presented by Simo & Rifai (1990) has been derived from a three field variational principle with displacement, strain and stress as independent variational parameters. Belytschko & Leviathan (1994) developed an assumed strain procedure using the Hu-Washizu varuational principle to stabilize the zero-energy modes of shell elements. Another common numerical technique that is widely used to deal with locking problems in the finite element analysis is the selective reduced integration (Zienkiewicz *et al.*, 1979) of strain energy terms, which was extended also to investigate the membrane locking in curved elements (Stolarski & Belytschko, 1982). For flat shell elements, the quasi-conforming technique (Kim *et al.*, 2003) is used for which the strains are discretized using a truncated Taylor series expansion, while the displacements are defined using string functions. Unlike most finite element approximation functions that interpolate the displacements within the element domain, the displacement approximation functions in the quasi-conforming technique are used to surface fit nodal displacement values within a problem domain. Carrera & Brischetto (2008) developed closed form solutions for a unified formulation to investigate the thickness locking for thin shell theory, first order shear deformation theory, higher order theories, mixed theories and layer-wise theories. Among their conclusions, they mentioned that the thickness locking appears, if and only if, transverse normal

strains are assumed constant and that it does not depend on geometrical curvature parameters.

An interesting approach to avoid locking in shell elements is the field consistent strain field approach, developed by Prathap (1985) to derive shear deformable shell elements. Inspired by the work of Mohr (1980, 1981), Prathap explored the origin of the locking problem by analyzing the true and spurious constraints of the discretized tangential membrane and transverse shear strains. As a result, the field consistent strains are derived and replace the original strains in the energy expressions. Many field consistent techniques were developed later such as the consistent polynomial order technique for shape functions (Koziey & Mirza, 1997), the discrete shear gap (Bletzinger *et al.*, 2000) and the discrete strain gap (Koschnick *et al.*, 2005) to mention a few. Those aforementioned formulations are almost identical to the reduced integration techniques, which prove the current success of implementing reduced integrations in commercial finite element packages to alleviate locking problems.

The previous models have been extended to model multilayered shell structures. As a few examples, Lee *et al.* (2002) investigated the dynamic characteristics of cylindrical composite panels with viscoelastic layers based on the partial layerwise theory. Nayak & Shenoi (2005) developed a family of assumed strain shell elements based on a refined higher order theory to analyze the natural frequencies of composite sandwich shells. Jeung & Shen (2001) extended the isoparametric degenerate shell element to model constrained layer damping treatments. Kulikov & Plotnikova (2006) presented a family of geometrically exact assumed stress–strain four-node curved solid-shell elements with six displacement degrees of freedom per node by using the first-order equivalent single-layer theory. Arciniega & Reddy (2005) developed a finite element model for a consistent third-order shell theory with applications to composite circular cylinders. A class of solid shell finite elements was formulated based on the application of the enhanced assumed strain method for linear (Alves de Sousa *et al.*, 2003), nonlinear (Fontes Valente *et al.*, 2004), and extended to layerwise nonlinear analysis (Moreira e*t al.*, 2010).

Discrete layer theories are known for their accuracy, especially for multilayered structures, since the displacement field is usually defined at the interfaces of the structure. Alam & Asnani (1984) developed a discrete layer theory for moderately thick shells to study the vibration and damping of a general multi-layered cylindrical shell having an arbitrary number of orthotropic material layers and viscoelastic layers. The discrete layer finite element model was then developed for shells (Ramesh & Ganesan, 1993 Wang & Chen, 2004), with limitation to circular cylindrical shapes using axisymmetric, circumferential wave numbers. In this paper, a discrete layer finite element model is derived for cylindrical shells and panels using a modified version of the consistent strain field approach. The element is basically a brick shell element

incorporating the plane stress assumption. Thus, it has the advantage of defining the inplane displacement field at the shell layer interfaces while reducing the size of the discretized shell problem via plane stress. The element can be easily extended to general shell configurations via simple modification of the kinematic equations.

THEORETICAL FORMULATION

This section describes the discrete layer formulation for a moderately thick shell under the plane stress assumption. Then, a field consistent finite element model is formulated for anisotropic composites.

Kinematics

For shells in a state of plane stress, the transverse (radial) displacement, w, is assumed constant through the thickness. The inplane axial and tangential displacements, u and v, for layer k are assumed to vary linearly across the thickness of the layer (see Figure 1). Hence the displacement field is defined by

$$
\begin{aligned}
u(x,y,z) &= \frac{1}{2}(u_k + u_{k+1}) + \frac{z}{t_k}(u_{k+1} - u_k) \\
v(x,y,z) &= \frac{1}{2}(v_k + v_{k+1}) + \frac{z}{t_k}(v_{k+1} - v_k) \\
w(x,y,z) &= w
\end{aligned}
\tag{1}
$$

The strain displacement relations for moderately thick cylindrical shells are given by

$$
\mathring{\mathbf{a}} = \begin{Bmatrix} \varepsilon_x \\ \varepsilon_y \\ \gamma_{xy} \end{Bmatrix}, \qquad \bar{\mathbf{a}} = \begin{Bmatrix} \gamma_{yz} \\ \gamma_{xz} \end{Bmatrix}
\tag{2}
$$

with the strain components defined by

$$
\begin{aligned}
\varepsilon_x &= \frac{\partial u}{\partial x}, \\
\varepsilon_y &= \frac{1}{1+z/r_k}\left(\frac{\partial v}{\partial y} + \frac{w}{r_k}\right), \\
\gamma_{xy} &= \frac{\partial v}{\partial x} + \frac{1}{1+z/r_k}\left(\frac{\partial u}{\partial y}\right) \\
\gamma_{yz} &= \frac{1}{1+z/r_k}\left(\frac{\partial w}{\partial y} - \frac{v}{r_k}\right) + \frac{\partial v}{\partial z}, \\
\gamma_{xz} &= \frac{\partial w}{\partial x} + \frac{\partial u}{\partial z}
\end{aligned}
\tag{3}
$$

Where $\boldsymbol{\varepsilon}$ and $\boldsymbol{\gamma}$ are the inplane strains and transverse shear strains, respectively, with r denoting the radius of curvature.

Constitutive model

For a shell composed of N orthotropic layers, the stresses in layer k are related to strains through

$$
\begin{Bmatrix} \sigma_x \\ \sigma_y \\ \tau_{xy} \end{Bmatrix} = \begin{bmatrix} \bar{Q}_{11} & \bar{Q}_{12} & \bar{Q}_{16} \\ \bar{Q}_{12} & \bar{Q}_{22} & \bar{Q}_{26} \\ \bar{Q}_{16} & \bar{Q}_{26} & \bar{Q}_{66} \end{bmatrix} \begin{Bmatrix} \varepsilon_x \\ \varepsilon_y \\ \gamma_{xy} \end{Bmatrix}, \qquad \begin{Bmatrix} \tau_{yz} \\ \tau_{xz} \end{Bmatrix} = \begin{bmatrix} \bar{Q}_{44} & \bar{Q}_{45} \\ \bar{Q}_{45} & \bar{Q}_{55} \end{bmatrix} \begin{Bmatrix} \gamma_{yz} \\ \gamma_{xz} \end{Bmatrix} \quad (4)
$$

or in vector form by

$$
\boldsymbol{\sigma} = \mathbf{C}\boldsymbol{\varepsilon}, \qquad \boldsymbol{\tau} = \mathbf{G}\boldsymbol{\gamma} \tag{5}
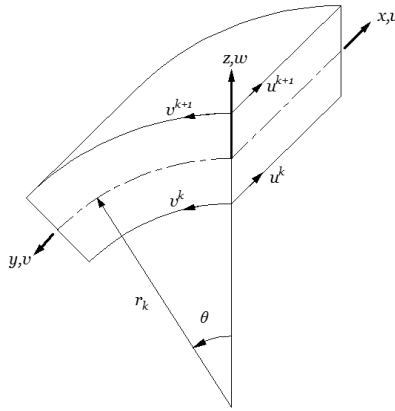$$

Fig. 1. Discrete layer shell element

where $\bar{Q}_{ij}$ are the transformed stiffness coefficients obtained from:

$$
\begin{aligned}
\bar{Q}_{11} &= Q_{11}\cos^4 q + Q_{22}\sin^4 q + 2(Q_{12} + 2Q_{66})\cos^2 q \, \sin^2 q \\
\bar{Q}_{22} &= Q_{11}\sin^4 q + Q_{22}\cos^4 q + 2(Q_{12} + 2Q_{66})\cos^2 q \, \sin^2 q \\
\bar{Q}_{12} &= Q_{12}(\cos^4 q + \sin^4 q) + (Q_{11} + Q_{22} - 4Q_{66})\cos^2 q \, \sin^2 q \\
\bar{Q}_{16} &= (Q_{11} - Q_{12} - 2Q_{66})\cos^3 q \, \sin q - (Q_{22} - Q_{12} - 2Q_{66})\sin^3 q \, \cos q \\
\bar{Q}_{26} &= (Q_{11} - Q_{12} - 2Q_{66})\sin^3 q \, \cos q - (Q_{22} - Q_{12} - 2Q_{66})\cos^3 q \, \sin q \\
\bar{Q}_{44} &= Q_{44}\cos^2 q + Q_{55}\sin^2 q \\
\bar{Q}_{55} &= Q_{55}\cos^2 q + Q_{44}\sin^2 q \\
\bar{Q}_{45} &= (Q_{55} - Q_{44})\sin q \cos q
\end{aligned} \tag{6}
$$

$$
\begin{aligned}
Q_{11} &= \frac{E_1}{1 - n_{12}n_{21}}, & Q_{12} &= \frac{n_{12}E_2}{1 - n_{12}n_{21}}, & Q_{22} &= \frac{E_2}{1 - n_{12}n_{21}} \\
Q_{66} &= G_{12}, & Q_{44} &= G_{23}, & Q_{55} &= G_{13}
\end{aligned}
$$

with E, G and n are Young's modulus, shear modulus and Poisson's ratio, respectively.

Bilinear shape functions

The proposed quadrilateral element has twenty degrees of freedom (dofs) with five dofs at each of the four corner nodes. The nodal dofs vector, $\boldsymbol{\delta}_i$, and the layer dofs vector $\boldsymbol{\delta}$ are defined as:

$$
\begin{aligned}
\boldsymbol{\delta}_i &= \left\{ U_i^k, U_i^{k+1}, V_i^k, V_i^{k+1}, W_i \right\} \\
\boldsymbol{\delta} &= \left\{ \boldsymbol{\delta}_1, \boldsymbol{\delta}_3, \boldsymbol{\delta}_3, \boldsymbol{\delta}_4 \right\}
\end{aligned}
\tag{7}
$$

Hence, the displacement shape functions are bilinear in x and y, and described by

$$
\begin{aligned}
u^k &= a_1 + a_2 x + a_3 y + a_4 xy \\
u^{k+1} &= a_5 + a_6 x + a_7 y + a_8 xy \\
v^k &= a_9 + a_{10} x + a_{11} y + a_{12} xy \\
v^{k+1} &= a_{13} + a_{14} x + a_{15} y + a_{16} xy \\
w &= a_{17} + a_{18} x + a_{19} y + a_{20} xy
\end{aligned}
\tag{8}
$$

Field consistent shape functions

It is very well known that shear deformable shell elements experience locking due to inconsistency of shape functions used to evaluate the strains. To clearly understand this issue, the discretized strain components will be analyzed for field inconsistency and consistent shape functions will be derived in a selective manner to enhance convergence and eliminate the excessive stiffening in the strain energy functional.

Membrane longitudinal strain e_x

The discretized strain is found by substituting the shape functions in e_x so that

$$
\begin{aligned}
\varepsilon_x &= \frac{\partial u}{\partial x} \\
&= \frac{1}{2}(a_2 + a_6) + \frac{1}{2}(a_4 + a_8)y + (a_6 - a_2)\frac{z}{t_k} + (a_8 - a_4)\frac{z}{t_k}y
\end{aligned}
\tag{9}
$$

It can be easily seen that this strain component has no locking issues since the strain is defined only from the longitudinal displacement, u. Hence, the four elements of strain in the last equation are consistently made from coefficients of both u^k and u^{k+1}. Notice that upon thickness integration, the final form of the discretized longitudinal strain is basically a linear function in the y direction.

Membrane tangential strain e_y

Substituting the shape functions in e_y given by

$$\varepsilon_y = \frac{1}{1+z/r_k}\left(\frac{\partial v}{\partial y}+\frac{w}{r_k}\right)$$

$$= \frac{1}{1+z/r_k}\{\ \frac{1}{2}(a_{11}+a_{15})+\frac{1}{2}(a_{12}+a_{16})x+(a_{15}-a_{11})\frac{z}{t_k}+(a_{16}-a_{12})\frac{z}{t_k}x \tag{10}$$

$$+\frac{1}{r_k}(a_{17}+a_{18}x+a_{19}y+a_{20}xy)\ \}$$

and integrating over the thickness, it can be readily shown that $\partial v/\partial y$ is a linear function of x. Therefore, the inconsistent terms are due to the y and xy terms (i.e. a_{19} and a_{20}), which are parts of the transverse displacement w. As a result, w is modified upon substitution in e_y to become

$$w = a_{17} + a_{18}x \tag{11}$$

Membrane shear strain g_{xy}

The discretized membrane shear strain is

$$\gamma_{xy} = \frac{\partial v}{\partial x}+\frac{1}{1+z/r_k}\left(\frac{\partial u}{\partial y}\right)$$

$$= \frac{1}{2}(a_{10}+a_{14})+\frac{1}{2}(a_{12}+a_{16})y+(a_{14}-a_{10})\frac{z}{t_k}+\frac{1}{2}(a_{16}-a_{12})\frac{z}{t_k}y \tag{12}$$

$$+\frac{1}{1+z/r_k}\left\{\frac{1}{2}(a_3+a_7)+\frac{1}{2}(a_4+a_8)x+(a_7-a_3)\frac{z}{t_k}+\frac{1}{2}(a_8-a_4)\frac{z}{t_k}x\right\}$$

Upon thickness integration, $\partial v/\partial x$ becomes a linear function of y while $\partial u/\partial y$ becomes a linear function of x. The consistent terms between $\partial v/\partial x$ and $\partial u/\partial y$ are the constant ones, rendering the coefficients of x and y in the last equation as field inconsistent. This suggests that the field consistent membrane shear strain should be just a constant, which can be achieved by eliminating the bilinear term xy from all inplane displacement shape functions as follows

$$u^k = a_1 + a_2 x + a_3 y$$
$$u^{k+1} = a_5 + a_6 x + a_7 y$$
$$v^k = a_9 + a_{10}x + a_{11}y \tag{13}$$
$$v^{k+1} = a_{13} + a_{14}x + a_{15}y$$

Transverse shear strains g_{xz} and g_{yz}

The shear strain γ_{xz} is given, after substitution of the shape functions, by the following relationship

$$\gamma_{xz} = \frac{\partial w}{\partial x}+\frac{\partial u}{\partial z}$$

$$= (a_{18}+a_5-a_1)+(a_{20}+a_7-a_3)y+(a_6-a_2)x+(a_8-a_4)xy \tag{14}$$

It can be seen that the constant term and the coefficient of *y,* both consist of components from *w* and *u,* while the coefficients of *x* and *xy* are made only of *u* components. Hence, in the Kirchhoff limits of vanishing shear strain, the constant coefficient and the coefficient of *y* are the true Kirchhoff constraints, while the other inconsistent coefficients of *x* and *xy* are spurious constraints from which the shear locking is generated. Hence, the consistent shear strain g_{xz} requires that the original shape functions of *u* are replaced by

$$u^k = a_1 + a_3 y$$
$$u^{k+1} = a_5 + a_7 y \tag{15}$$

By applying the field consistency procedure and integrating over the thickness, it can also be concluded that the field consistent g_{yz} is a linear function of *x*, which requires that the original shape functions of *v* are replaced by

$$v^k = a_9 + a_{10} x$$
$$v^{k+1} = a_{13} + a_{14} x \tag{16}$$

Like most other techniques that try to overcome locking problems, the present field consistent technique is not variationally consistent. The variational consistency requires that the strain compatibility equations must be satisfied (Ausserer & Lee, 1988) which is not a straight forward task for 2-D and 3-D shell structures. In fact, the present technique is always variationally correct if the strains are uncoupled. For example, the shear strains for isotropic materials and cross-ply orthotropic composites are always uncoupled, and hence the shear strain energy is always variationally correct under the present approach except for angle-ply composites. Even though the variational consistency is not totally satisfied, the proposed field consistent approach gives good results for angle-ply composites as will be shown later in the paper.

Variational equations of motion

The extended Hamilton's principle is used to derive the kinetic energy, *T*, potential energy, *U,* and work done, *W,* such that:

$$\int_{t_1}^{t_2} (dT - dU + dW) dt = 0 \tag{17}$$

where the variational terms are defined by

$$dT = r \int_{V_e} (du^T \& u \& + dv^T \& v \& + dw^T \& w \& dV)$$

$$dU = \int_{V_e} (d\varepsilon^T \mathbf{C}\varepsilon + d\gamma^T \Gamma\gamma) dV \tag{18}$$

$$dW = \int_{S} (dw f_z + dv f_y + du f_x) dS$$

with f_i is defined as the *i* direction load applied on the surface *S* of the shell. Note that *S* and *V* are defined in the exact geometric sense were

$$dS = \frac{1}{1 + z/r_k} dxdy$$
$$dV = \frac{1}{1 + z/r_k} dxdydz$$

(19)

Minimizing the Hamilton's principle for the discretized problem domain, the global dynamic equation of motion becomes

$$\mathbf{M}\ddot{\Delta} + \mathbf{K}\Delta = \mathbf{F}$$

(20)

Where **M** and **K** are the mass and stiffness matrics, while **F** and Δ are the force and discplacement vectors, respectively. For harmonic motion, the eigenvalue problem is obtained by assuming $\bar{\Delta} = \Delta e^{iwt}$, hence

$$(\mathbf{M}w^2 - \mathbf{K})\bar{\Delta} = 0$$

(21)

while for static response, the mass matrix is omitted from the equation of motion resulting in

$$\mathbf{K}\Delta = \mathbf{F}$$

(22)

Numerical validation

In this section, the current shell discrete layer element is tested against existing standard shell finite elements via a set of static and dynamic problems. Two different elements will be used to evaluate the performance of the discrete layer shell element. The first element is the standard discrete layer shell element (SDLE) which implements all the modified shape functions. The second element (SDLEx) implements all the modified shape functions, except the shape functions of the membrane shear strain remain unchanged. In some examples, SDLE and SDLEx give almost typical results, and hence only SDLE is compared against other elements.

Pinched cylinder

The pinched cylinder is a well known benchmark for testing the ability of shell finite elements to model the state of inextensional bending. The cylinder is subjected to a *unit* point load *p* at the center on opposite sides of the cylinder, as shown in Figure 2, and has rigid end diaphragms ($v = w = 0$). Since the problem is symmetric, only one octant of the cylinder is used. The geometric and material properties of the cylinder are

$E = 3 \times 10^6$, $n = 0.3$, $r = 300$, length $= 600$.

The performance of the new element is compared to MITC4 (Dvorkin & Bathe, 1984), the enhanced assumed strain element by Simo *et al.* (1989) and XSHELL41 by Kim *et al.* (2003)
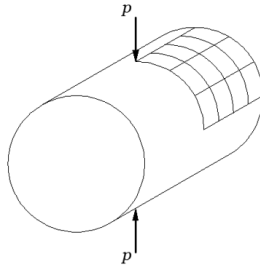

Fig. 2. The pinched cylinder problem

Table 1. Convergence of the normalized deflection for the pinched cylinder problem

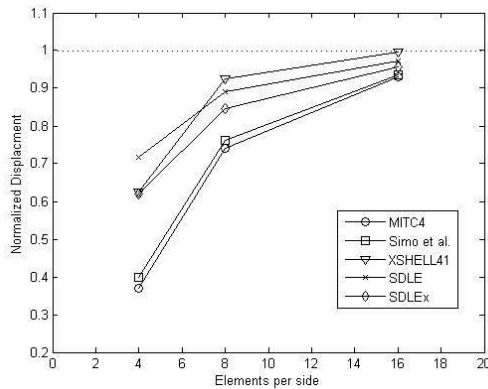| Mesh	MITC4	Simo *et al.*	XSHELL41	SDLE	SDLEx
4×4	0.37	0.399	0.625	0.7179	0.6194
8×8	0.74	0.763	0.926	0.8896	0.8467
16×16	0.93	0.935	0.995	0.9713	0.9569

Fig. 3. Convergence of the radial displacement at the location of the load for the pinched cylinder problem

The reference value of the radial displacement at the location of the load is 1.8248×10^{-5}. Both proposed elements have shown good convergence to the reference solution, with SDLE outperforming SDLEx.

Scordelis-Lo roof

The Scordelis-Lo roof, shown in Figure 4, is another standard benchmark for testing the ability of shell finite elements to model membrane dominated problems. The

cylindrical panel is subjected to its own gravitational load q (acting vertically down, not radially) and has rigid diaphragms at the curved edges ($v = w = 0$), with the other straight ends free. Only one quarter of the cylinder is used due to symmetry. The geometric and material properties of the panel are

$E = 4.32 \times 10^8$, $n = 0.0, r = 25, \theta = 40^{\circ}$, length $= 50, q = -90$

The vertical displacement at the center of the free end, point A, is determined and the solution is compared against other shell elements as shown in Table 2. The reference value used here is 0.3024 (MacNeal & Harder, 1985), which is used by many finite element packages. The SDLEx shows poor convergence with respect to all other elements, while SDLE is showing competitive performance. It should be noted here that the SDLE converges to a value of 0.3080 which is very close to the theoretical solution value of 0.3086.

Table 2. Convergence of the normalized deflection for the Scordelis-Lo roof problem

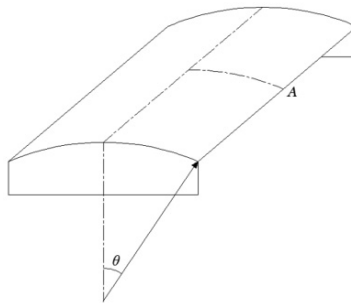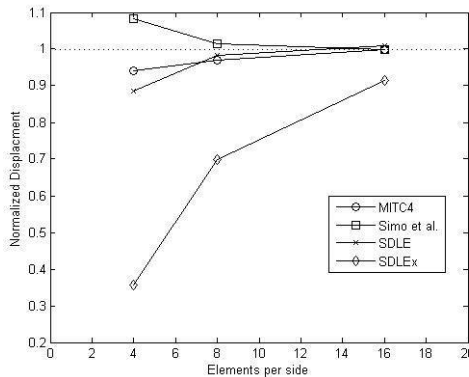| Mesh	MITC4	Simo *et al.*	SDLE	SDLEx
4×4	0.94	1.083	0.8857	0.3562
8×8	0.98	1.015	0.9820	0.6984
16×16	1.01	1.000	1.0091	0.9142

Fig. 4. Scordelis-Lo roof

Fig. 5. Convergence of the vertical displacement at point A of the Scordelis-Lo roof shell problem

Bending of laminated composite cylindrical panel

This problem deals with a cross-ply laminated cylindrical panel that is simply supported at all its edges (i.e. $v = w = 0$ on curved edges and $u = w = 0$ on straight edges). The panel has a total angle of θ, mean radius r, length a, width $b = r\theta$, thickness h and it is subjected to a sinusoidally distributed transverse load f_z. The geometric and material properties of the composite panel are

$$E_1 = 25E_2, \qquad G_{12} = G_{13} = 0.5E_2, \ G_{23} = 0.2E_2, \ n_{12} = 0.25$$

$$r = 1, \ \theta = \pi/4 \text{ rad}, \ a = 4, \ f_z = q \sin\frac{px}{a} \sin\frac{py}{b}$$

The non dimensional displacement, $\bar{w} = 10wE_1h^3 / qr^3$, is calculated at the center of the panel and compared with other existing results reported in Chang *et al.* (2000) and Reddy (2003), as shown in Table 3. The SDLE shows good comparable results with other references, with all the SDLE results higher than those of their counterparts. The highest discrepancy occurs for the smallest r/h and for an increasing number of laminated layer mismatch (90/0/90). This discrepancy might be due to the flexibility of the current discrete layer approach in comparison with the classical lamination approach of the other two references.

Vibrations of thin orthotropic circular cylindrical shells

This problem is concerned with the free vibrations of a thin orthotropic circular cylindrical shell. The circular shell is clamped from both sides and has the following geometric and material properties

$$E = 204 \times 10^9, \qquad n = 0.29, \qquad \rho = 7833, \quad r = 0.0762, \text{ length} = 0.3048, \ h = 0.0254$$

The modal frequencies in terms of the longitudinal mode m and circumferential mode n are compared with the exact characteristics solution of the thin shell (Liu *et al.*, 2012) as shown in Table 4. While both elements give good results in general, the SDLEx gives slightly more accurate results for higher circumferential modes.

Vibrations of thin laminated composite circular cylindrical shell

A composite version of the previous example is validated here, where only the fundamental frequencies are calculated. The problem at hand is a clamped laminated composite circular shell with mean radius r, total thickness h (equally distributed on plies) and has the following geometric and material properties

$$E_1 = 206.9, \qquad E_2 = E_3 = 18.62, \ G_{23} = G_{23} = G_{23} = 4.48, \ n_{12} = n_{13} = n_{23} = 0.28$$

$$r = 0.1905, \ h = 0.000501, \text{ length} = 0.381$$

Both angle-ply and cross-ply laminated composite shells are used in this problem. The results of the present SDLE and SDLEx are compared in Table 5 with results from the classical shell theory (Sheinman & Greif, 1984) and a double superposition global-local theory (Shariyat, 2011). Both elements give good results within the range of both mentioned references.

Vibrations of moderately thick laminated composite circular cylindrical panels

The fundamental frequencies of moderately thick cross-ply laminated cylindrical panels are calculated in this example for different boundary conditions. The panels have both their straight edges simply supported ($u = w = 0$), while the curved edges are subjected to different sets of Free (F), Clamped (C) and Simply-Supported (S) conditions. The panel has a mean radius r, length a, width b, and total thickness h (equally distributed on plies). The material properties of the composite panel are:

$$E_1 = 25E_2, \qquad G_{12} = G_{13} = 0.5E_2, \; G_{23} = 0.2E_2, \; n_{12} = 0.25, \; a/h = 10, \; a/b = 1.$$

The non dimensional fundamental frequency, $\bar{l} = l\,a^2\sqrt{r / E_2 h^2}$, for the SDLE is compared with theoretical results by Messina & Soldatos (1999), referred as MS, and also by Khdeir & Reddy (1990), referred as KR, as shown in Table 6. The SDLE shows good results with a maximum discrepancy of 9%. This maximum discrepancy occured for the smallest r/h, for an increasing number of laminated layer mismatch (90/0/90), and for the clamped boundary condition, which is the fully constrained condition. The SDLE underestimates the frequencies for constrained conditions and the underestimation increases as the degree of constraining increases. In other words, for relatively less constrained conditions, the discrepancy between the SDLE and the other references decreases. This discrepancy confirms that the discrete layer approach is more flexible than other common approaches.

Table 3. Displacements at the center of the laminated cross ply panel

	90/0/90			0/90		
r/h	Cheng *et al.*	Reddy	SDLE	Cheng *et al.*	Reddy	SDLE
50	0.5486	0.5458	0.5634	2.2372	2.2586	2.2874
100	0.4711	0.4718	0.4765	1.3666	1.3720	1.3815
500	0.1027	0.1028	0.1030	0.1005	0.1006	0.1008

Table 4. Frequencies (Hz) of the present DLFE elements compared with exact results

m/n		1	2	3	4	5	6	7	8
1	SDLE	3424	1913	1149	758	576	540	610	750
	SDLEx	3425	1916	1153	764	583	546	615	753
	Exact	3425	1917	1154	764	580	538	598	723
2	SDLE	6413	3899	2527	1740	1274	1014	910	932
	SDLEx	6415	3903	2535	1750	1288	1029	925	946
	Exact	6412	3903	2537	1752	1287	1022	907	911
3	SDLE	8497	5840	4042	2901	2167	1696	1414	1286
	SDLEx	8499	5845	4052	2916	2187	1720	1440	1312
	Exact	8493	5841	4052	2920	2191	1720	1431	1287
4	SDLE	9426	7303	5437	4082	3136	2482	2041	1772
	SDLEx	9427	7308	5448	4100	3161	2513	2077	1810
	Exact	9420	7299	5444	4102	3167	2518	2077	1797

Table 5. Fundamental frequencies (Hz) of the clamped cylindrical laminated shells

Orientation	Sheinman and Greif	Shariyat	SDLE	SDLEx
0/0/0	261.3	266.31	260.36	261.34
15/0/15	316.0	321.74	315.54	318.34
30/0/30	376.8	381.15	376.48	384.58
45/0/45	420.0	425.62	421.22	430.93
60/0/60	424.3	433.34	425.10	431.81
75/0/75	395.0	401.83	394.82	398.15
90/0/90	370.5	374.87	369.69	370.36
15/0/-15	333.1	342.27	331.49	333.62
30/0/-30	362.2	371.85	366.95	370.38
45/0/-45	362.4	369.26	368.44	373.03
60/0/-60	379.7	384.95	383.52	387.20
75/0/-75	393.8	397.87	394.45	396.40

Table 6. Fundamental frequencies (Hz) of the laminated composite panel

Orientation	r/a		SS	SC	CC	FF	FS	FC
0/90	5	MS	8.987	13.860	13.095	5.741	6.056	6.557
		KR	9.024	13.866	13.119	5.700	5.101	6.600
		SDLE	9.031	12.800	12.655	5.779	6.113	6.608
	20	MS	8.967	10.841	13.070	5.809	6.133	6.588
		KR	8.973	10.871	12.070	5.800	6.139	6.594
		SDLE	8.923	10.707	12.593	5.773	6.105	6.553
0/90/0	5	MS	11.839	13.860	16.023	3.767	4.298	6.114
		KR	11.846	13.866	16.028	3.783	4.312	6.123
		SDLE	11.213	12.800	14.583	3.757	4.281	5.950
	20	MS	11.793	13.825	15.999	3.789	4.323	6.089
		KR	11.793	13.825	15.999	3.789	4.322	6.089
		SDLE	11.163	12.760	14.552	3.779	4.307	5.926

CONCLUSION

A discrete layer finite element is proposed in this paper to model thin and moderately thick cylindrical shells. The element has twenty degrees of freedom, five at each of the four corner nodes. A consistent field approach is implemented to eliminate the various locking phenomena due to membrane shear strain, in-plane tangential strain, and transverse shear strains. The field consistent strains are obtained by omitting the inconsistent terms from the original displacement shape functions. The element has been validated through standard benchmark tests with good convergence rate and accurate results. In addition to the field consistency of transverse shear and membrane tangential strains, faster converging results have been noticed, when the membrane shear strain is also field consistent, and more significantly for problems that include membrane loads like the famous Scordelis-Lo roof. As the number of mismatched laminated composite layers increase, the element produces higher displacements for the static bending analysis and lower natural frequencies for the free vibration analysis. In addition, the discrepancy increases by increasing the degree of boundary constraining. This confirms that the current shell discrete layer element has more flexibility than the other approaches due to the fact that the inplane displacement field is defined on the element interfaces, rather than the midsurface as done in the equivalent single

layer and layerwise theories. This suggests that the shell discrete layer theory under consideration should be analyzed and compared against other existing shell theories for additional understanding of the advantages and disadvantages of the discrete layer approach.

ACKNOWLEDGMENT

REFERENCES

Ahmad, S., Irons, B.M. & Zienkiewicz, O.C. 1970. Analysis of thick and thin shell structures by curved finite elements. International Journal for Numerical Methods in Engineering 2: 419-451.

Alam, N. & Asnani, N.T. 1984. Vibration and damping analysis of a multilayered cylindrical shell, Part I: theoretical analysis. AIAA Journal 22: 803-810.

Alves de Sousa, R.J., Natal Jorge, R.M., Fontes Valente, R.A. & César de Sá, J.M.A. 2003. A new volumetric and shear locking-free 3D enhanced strain element. Engineering Computations 20: 896-925.

Arciniega, R.A. & Reddy, J.N. 2005. Consistent third-order shell theory with application to composite circular cylinders. AIAA 43: 2024-2038.

Ashwell, D.G. & Sabir, A.B. 1972. A new cylindrical shell finite element based on simple independent strain functions. International Journal for Mechanical Sciences 14: 171-183.

Ausserer, M.F. & Lee, S.W. 1988. An eighteen node solid element for thin shell analysis. International Journal for Numerical Methods in Engineering 26: 1345-1364.

Belytschko, T. & Leviathan, I. 1994. Physical stabilization of the 4-node shell element with one point quadrature. Computer Methods in Applied Mechanics and Engineering 113:321-350.

Bletzinger, K.U., Bischoff, M. & Ramm, E. 2000. A unified approach for shear-locking-free triangular and rectangular shell finite elements. Computers and Structures 75: 321-334.

Bogner, F.K., Fox, R.L. & Schmit, L.A. 1967. A cylindrical shell discrete element. AIAA Journal 5: 745-750.

Carrera, E. & Brischetto, S. 2008. Analysis of thickness locking in classical, refined and mixed theories for layered shells. Composite Structures 85: 83-90.

Cheng, Z.Q., He, L.H. & Kitipornaci, S. 2000. Influence of imperfect interfaces on bending and vibration of laminated composite shells. International Journal of Solids and Structures 37: 2127-2150.

Connor, J.J. & Brebbia, C. 1967. Stiffness matrix for shallow shell rectangular shell element. Proceedings of the American Society of Civil Engineers, Journal of Engineering Mechanics 93: 43-65.

Djoudi, M.S. & Bahai, H. 2004. A cylindrical strain-based shell element for vibration analysis of shell structures. Finite Elements in Analysis and Design 40: 1947 -1961.

Dvorkin, E.N. & Bathe K.J. 1984. A continuum mechanics based four-node shell element for general non-linear analysis. Engineering Computations 1:77-88.

Fontes Valente, R.A., Alves de Sousa, R.J. & Natal Jorge, R.M. 2004. An enhanced strain 3D element for large deformation elastoplastic thin-shell applications. Computational Mechanics 34: 38-52.

Hrennikoff, A. & Tezcan, S.S. 1966. Analysis of cylindrical shells by the finite element method.

Symposium on Problems of Interdependence of Design and Construction of Large-Spam Shells for Industrial and Civic Buildings, Leningrad, USSR.

Jeung, Y.S. & Shen, Y. 2001. Development of isoparametric, degenerate constrained Layer element for plate and shell structures. AIAA Journal 39: 1997-2005.

Khdeir A.A. & Reddy JN. 1990. Influence of edge conditions on the modal characteristics of cross-ply laminated shells. Computers and Structures 34: 817-826.

Kim, K.D., Lomboy, G.R. & Voyiadjis, G.Z. 2003. A 4-node assumed strain quasi-conforming shell element with 6 degrees of freedom. International Journal for Numerical Methods in Engineering 58: 2177-2200.

Koschnick, F., Bischoff, M., Camprub, N. & Bletzinger, K.U. 2005. The discrete strain gap method and membrane locking. Computer Methods in Applied Mechanics and Engineering 194:2444-2463.

Koziey, B.L. & Mirza, F.A. 1997. Consistent thick shell element. Computers and Structures 65:531-549.

Kulikov, G.M. & Plotnikova, S.V. 2006. Geometrically exact assumed stress-strain multilayered solid-shell elements based on the 3D analytical integration. Computers and Structures 84: 1275-1287.

Lee, I., Oh, I.K., Shin, W.H., Cho, K.D. & Koo, K.N. 2002. Dynamic characteristics of cylindrical composite panels with co-cured and constrained viscoelastic layers. JSME Internatioal Journal Series C 45:16-25.

Liu, B., Xing, Y.F., Qatu, M.S & Ferreira A.J.M. 2012. Exact characteristic equations for the free vibrations of thin orthotropic circular cylindrical shells. Composite Structures 94: 484-493.

MacNeal, R.H. 1982. Derivation of element stiffness matrices by assumed strain distributions. Journal of Nuclear Engineering Design 70:3-12.

MacNeal, R.H. & Harder, R.L. 1985. A proposed standard set of problems to test finite element accuracy. Finite Elements in Analysis and Design 1: 3-20.

Messina, A. & Soldatos, K.P. 1999. Influence of edge boundary conditions on the free vibratrions of cross-ply laminated circular cylindrical panels. Journal of the Acoustical Society of America 106: 2608-2620.

Mohr, GA. 1980. Numerically integrated triangular element for doubly curved thin shells. Computers and Structures 11: 565-571.

Mohr, G.A. 1981. A doubly curved isoparametric triangular shell element. Computers and Structures 14: 9-13.

Moreira, R.A.S., Alves de Sousa, R.J. & Fontes Valente, R.A. 2010. A solid-shell layerwise finite element for non-linear geometric and material analysis. Composite Structures 92: 1517-1523.

Nayak, A.K. & Shenoi, R.A. 2005. Free Vibration Analysis Of Composite Sandwich Shells Using Higher Order Shell Elements. 46th AIAA/ASME/ASCE/AHS/ASC Structures, Structural Dynamics and Materials Conference, Austin, Texas.

Prathap, G. 1985. A C0 continuous four-noded cylindrical shell element. Computers and Structures 21: 995-999.

Ramesh, T.C. & Ganesan, N. 1993. Vibration and damping analysis of cylindrical shells with a constrained damping layer. Computers and Structures 46: 751-758.

Reddy JN. 2003. Mechanics of laminated composite plates and shells; Theory and analysis. CRC Press, Boca Raton, FL, USA.

Shariyat M. 2011. An accurate double-superposition global-local theory for vibration and bending analyses of cylindrical composite and sandwich shells subjected to thermo-mechanical loads. Proceedings of the Institution of Mechanical Engineers. Part C: Journal of Mechanical Engineering Sciences 225: 1816-1832.

Sheinman, I. & Greif, S. 1984. Dynamic analysis of laminated shells of revolution. Journal of Composite Materials 18: 200-215.

Simo, J.C. & Fox, D.D. & Rifai, M.S. 1989. On stress resultant geometrically exact shell model. Part II: the linear theory; computational aspects. Computer Methods in Applied Mechanics and Engineering 73:53-92.

Simo, J.C. & Rifai, S. 1990. A class of mixed assumed strain methods and the method of incompatible models. International Journal for Numerical Methods in Engineering 29:1595-1638.

Stolarski, H. & Belytschko, T. 1982. Membrane locking and reduced integration for curved elements. Journal of Applied Mechanics 49:172-176.

Wang, H.J. & Chen, L.W. 2004. Finite element dynamic analysis of orthotropic cylindrical shells with a constrained damping layer. Finite Elements in Analysis and Design 40: 737-755.

Zienkiewicz, O.C. & Cheung, Y.K. 1966. Plate and shell problems, finite element displacement approach. International Symposium on the Use of Electrical Digital Computers in Structural Engineering, Newcastle, UK.

Zienkiewicz, O.C., Taylor, R.L. & Too JM. 1979. Reduced integration techniques in general analysis of plates and shells. International Journal for Numerical Methods in Engineering 3:275-290.